PHYSICAL REVIEW C VOLUME 16, NUMBER 6 DECEMBER 1977

Deexcitation gamma rays from the interaction of 70-MeV pions with s-d shell nuclei*

M. Zaider,† D. Ashery, S. Cochavi, S. Gilad, M. A. Moinester, Y. Shamai, and A. I. Yavin
Tel-Aviv University, Ramat-Aviv, Israel
and Centre d'Etudes Nucléaires de Saclay, France
(Received 7 July 1976; revised manuscript received 21 June 1977)

The interaction of 70-MeV positive and negative pions with s-d shell nuclei was studied via measurements of the deexcitation γ rays from residual nuclei produced in the reactions. Cross sections for producing specific levels in the residual nuclei were measured. The results are compared with Monte Carlo calculations of intranuclear cascades, followed by evaporation processes. In order to take into account the special features of the prompt γ-ray technique, the probability for leaving the residual nuclei at different regions of excitation, together with measured γ-ray branching ratios, are incorporated into the calculated cross sections. Good agreement is found between measured and calculated cross sections for reactions involving the removal of four or more nucleons. For such reactions, the calculations are dominated by pion absorption processes. The cross sections for the removal of an α-equivalent cluster from T = 0 nuclei have about the same strength as those corresponding to the removal of a triton cluster from the neighboring $T = 1/2$ nuclei. This suggests that the final nucleus, rather than the removed particle, is mainly responsible for the observed strength. The cross sections for single-nucleon-removal reactions do not agree with the calculations.

[NUCLEAR REACTIONS ^{23}Na, Mg, ^{27}Al, ^{28}Si, ^{31}P, ^{32}S, ^{39}K, ^{40}Ca ($\pi^{\pm}$, $\chi\gamma$), E_{π} = 70 MeV, Ge(Li) detector, measured cross sections for producing specific levels in residual nuclei, calculated σ.]

I. INTRODUCTION

The prompt γ-ray technique has been used extensively in the last few years for the investigation of the interactions of pions with nuclei. In this technique, the deexcitation γ rays from the final nuclei which are produced in the interaction are measured. Various reaction channels and their relative strengths are identified in this way, and cross sections are determined for specific final levels. In most cases it is difficult to know whether these levels are populated directly or via electromagnetic cascades from higher states. Also, no direct information about the outgoing particles is obtained.

Prompt γ-ray experiments have been performed over a wide range of targets and pion energies.[1-5] The main features found in these experiments can be summarized as follows:

(a) For reactions involving the removal of one nucleon from the target, the cross-section ratios of the type

$$R_1(A) = \frac{\sigma[A(\pi^-, \pi^- n)B]}{\sigma[A(\pi^+, \pi^+ n + \pi^0 p)B]}$$

were found to be considerably smaller than the values expected from impulse-approximation estimates. Similar results have been found previously in activation[6] experiments.

(b) For even-even target nuclei, large cross sections were found for reactions leading to final nuclei which differ from the target nucleus by an integral number of $(2p2n)$ equivalent clusters. These were referred to as "α" removal reactions. It was suggested[2] that these enhanced cross sections may be understood if α clusters are assumed to exist on the nuclear surface and a direct π-α interaction takes place.

(c) The distribution of final nuclei follows, as a general rule, the line of β stability.

An attempt[7] to interpret the results of these experiments in terms of intranuclear cascade-evaporation processes was made. In this study the features of the prompt γ-ray technique (see Sec. IV) were not taken into account in the calculations and the agreement with the experimental results was not satisfactory. Recently, Lieb *et al.*[8] modified the results of the cascade-evaporation calculations and obtained improved agreement.

In the present paper we report the results of prompt γ-ray experiments in which the interactions of 70-MeV positive and negative pions with ^{23}Na, Mg, ^{27}Al, ^{28}Si, ^{31}P, ^{32}S, ^{39}K, and ^{40}Ca nuclei were studied. The aim of the present work was to study, in a systematic way, the interactions of pions with s-d shell nuclei and to gain some insight into the reaction mechanisms. This was done by comparing the data with intranuclear-cascade-evaporation calculations, appropriately modified for prompt γ-ray experiments. The comparison between the results obtained for neighboring $T = \frac{1}{2}$ and $T = 0$ target nuclei yielded information on additional features of these reactions.

II. EXPERIMENTAL PROCEDURE

The experiments reported in this paper were performed using the secondary pion beam at the Saclay electron linear accelerator. Because of the low duty cycle of this beam (2%), we limited the average beam intensity to about 10^5 pions/sec. The pion beam intensity was monitored and found to be steady within each run to 5%. The 70-MeV pion beam had an energy spread of ±5%. Whenever the beam polarity was changed, the beam profile was checked using a plastic-scintillator hodoscope. The beam profile had a Gaussian shape with horizontal and vertical full width at half maximum (FWHM) of 5 and 2 cm, respectively.

The electron and muon contamination in the beam had previously been measured at Saclay.[9] The proton contaminant was eliminated using aluminum absorbers placed at the exit of the pion channel. The experimental layout is shown in Fig. 1. The γ-ray spectrometer was a 65-cm^3 Ge(Li) detector. The plastic scintillators $P1$ and $P2$ formed a beam telescope. They were placed 50 cm in front of the target, and they determined the beam intensity on target. A third plastic scintillator, $P3$, was placed on the front face of the Ge(Li) detector and was used in anticoincidence mode to eliminate background from charged particles which penetrated the γ detector. The target was inclined by about 40° to the beam axis. The Ge(Li) detector was placed at 110° to the beam axis thereby minimizing the flux of scattered pions hitting the detector. Lead shielding protected the Ge(Li) detector from the muons coming from decaying pions. The optimum distance between the center of the target and the Ge(Li) detector was found to be about 11 cm. A sheet of 2-mm thick lead was placed on the Ge(Li) detector in order to reduce the flux of low energy γ rays. The targets (about 11×11 cm^2) consisted of natural material in solid or powder form. Except for Mg where the ^{24}Mg abundance is 79%, the abundance of the main isotope in all other targets was greater than 92%. The targets were typically 2–3 g/cm^2 thick.

A simplified diagram of the electronic system is shown in Fig. 2. The γ-ray spectra were recorded in coincidence with the incident pions. This coincidence requirement of about 8-nsec FWHM resolution improved significantly the peak-to-background ratio in the γ-ray spectrum. The electronic system was designed to handle dead-time losses due to the high instantaneous counting rate in the pion telescope and in the γ-ray detector. The pion beam intensity was limited in order to keep the overall dead-time losses smaller than 15%. Dead-time losses were presumably a major factor for the large differences in published values[10] of absolute cross sections obtained in several

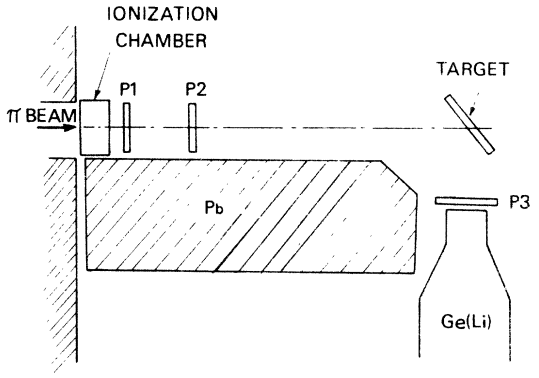

FIG. 1. General layout of the experimental setup.

prompt γ-ray experiments. We therefore describe here in some detail our system for dead-time measurement. The pion losses were measured as follows: Light emitting diodes (LED) were attached to the $P1$ and $P2$ plastic scintillators. The LED's were triggered by a pulse which was coincident with the pion beam, once every 4096 bursts. A known number of "pions" was simulated in this way. In order to distinguish between LED coincidences and $P1$-$P2$ coincidences produced by pions passing through the scintillators, two identical delays (of about 10 nsec each) were placed, one ($d1$) before $P1$ and the other ($d2$) after $P2$ (see Fig. 2). The outputs of the $P1$ and $P2$ detectors were simultaneously fed into two coincidence units (COIN1 and COIN2) each with a resolving time 2τ = 4 nsec. In this way COIN1 recorded only real pions, whereas COIN2 recorded only LED coincidences. In order to eliminate random coincidences generated by the incoming pions and recorded by COIN2, an additional coincidence from the pulse which triggered the LED's was required on the COIN2 unit. Whenever one of the LED pulses found the system blocked (due to a preceding pion), no LED coincidence was recorded. By comparing the number of LED coincidences with the number of LED triggers, the percentage loss of real pions in the beam was determined.

The same pulse which triggered the LED's also triggered an analog pulser, the output of which was

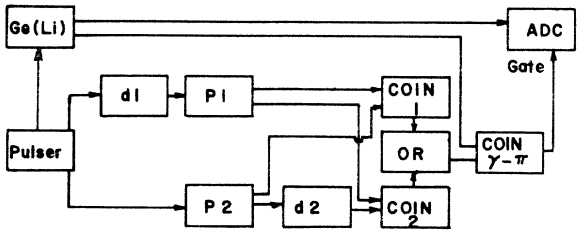

FIG. 2. Simplified block diagram of the electronic system.

then fed into the Ge(Li) preamplifier. In this way, a simulated "γ ray" was associated with the LED "pion." This "γ-ray" pulse passed through the same electronic system as any real γ-ray pulse and was recorded in the γ spectrum as a separate peak. The integrated counts in this "pulser peak" divided by the number of LED coincidences (COIN2) determined the live time in the γ detection system. The dead-time system was checked by performing three measurements in which the same target was bombarded at three different beam intensities. Calculated cross sections from the three measurements were consistent with one another. More details about the electronic system can be found elsewhere.[11]

The energy calibration of the Ge(Li) detector was done with radioactive sources of known γ-ray energies. The final calibration was made for each target separately using strong known γ lines in the spectra. The γ-ray detection efficiency included the intrinsic detector efficiency, γ-ray absorption in the target and geometric solid angle. This efficiency was measured using calibrated radioactive sources, and corrected for the effects of the nonuniform beam profile.

A typical measurement for each target lasted 3 h. A no-target measurement was performed in order to determine background lines. Room background was negligible due to the requirement of coincidence with incident pions. Most of the observed background was produced by the interaction of the beam or associated neutrons with the shielding and the Ge(Li) detector. A check for contribution to the measured spectra from electrons present in the beam was made by reducing the accepted beam momentum to the minimum. The beam consisted then practically of electrons only, and as expected, no contribution to the spectra was observed.

III. RESULTS

Examples of spectra following the interaction of π^+ and π^- with a sulphur target are shown in Fig. 3. The measured cross sections and γ-ray energies are presented in Table I. Most of the listed γ-ray energies correspond to ground state transitions. The "removed equivalent particle" indicates the cluster, or the corresponding group of individual nucleons, removed in the reaction, assuming inelastic pion scattering. This convention will be used in the rest of this section. This definition is less appropriate for Mg due to the low abundance of ^{24}Mg in the target.

Our criterion for γ-ray assignments was that the observed and known[12] energies agree to within the 2 keV uncertainty in the energy calibration and the uncertainty in the published values. γ lines, common to all targets (including measurement in C and O targets), were considered background. Also, if a level had two detectable branches, both transitions had to be observed, within the limits of the measured statistical accuracy. No levels with lifetimes longer than about 10 nsec were assigned. In some cases, more than one residual nucleus was assigned to the same γ-ray energy, as indicated in the table. Some assignments were checked against other types of measurements on the same target[13] (short and long lifetime activity measurements). We quote every assignment compatible with these criteria.

The cross sections for the observed transitions were calculated using the measured target thicknesses, detection efficiency, pion flux, dead-time losses, and beam contaminants. Each γ peak was integrated, and an average smooth background was subtracted. Overlapping peaks were unfolded using a standard shape taken from a strong, isolated peak. Peaks broadened significantly by the Doppler effect were not analyzed in this work.

In calculating the cross sections we assumed that γ rays are emitted isotropically. This assumption is justified since the incoming pion carries a relatively small amount of angular momentum. If, furthermore, many nucleons are emitted, any nuclear orientation is expected to be washed out. For an $E1$ transition following inelastic pion scattering (probably the most unisotropic case) only a 30% correction is required.[14]

The errors shown in Table I for the cross sections are due to statistics and to the uncertainties in the energy dependence of the detector efficiency. Thus, they determine the uncertainty in the relative intensities of different γ lines for π^+ or for π^- induced reactions. The absolute cross sections have an uncertainty of 15% due to systematic errors in the beam contamination, the dead-time corrections, and the absolute efficiency measurements.

An additional uncertainty present in some reactions is due to secondary reactions such as (n, n'), $(n, 2n)$, or (n, a) induced by neutrons produced in the target by the incoming pions. The contribution of these processes is difficult to estimate. An estimate based on measured neutron induced cross sections and calculated neutron yields in the target shows that (n, n') reactions could contribute up to 50% to the observed (π, π') cross sections, while (n, a) will have at most a 20% contribution to the "^{3}He" removal cross sections. The effect of the $(n, 2n)$ reaction was found to be small.

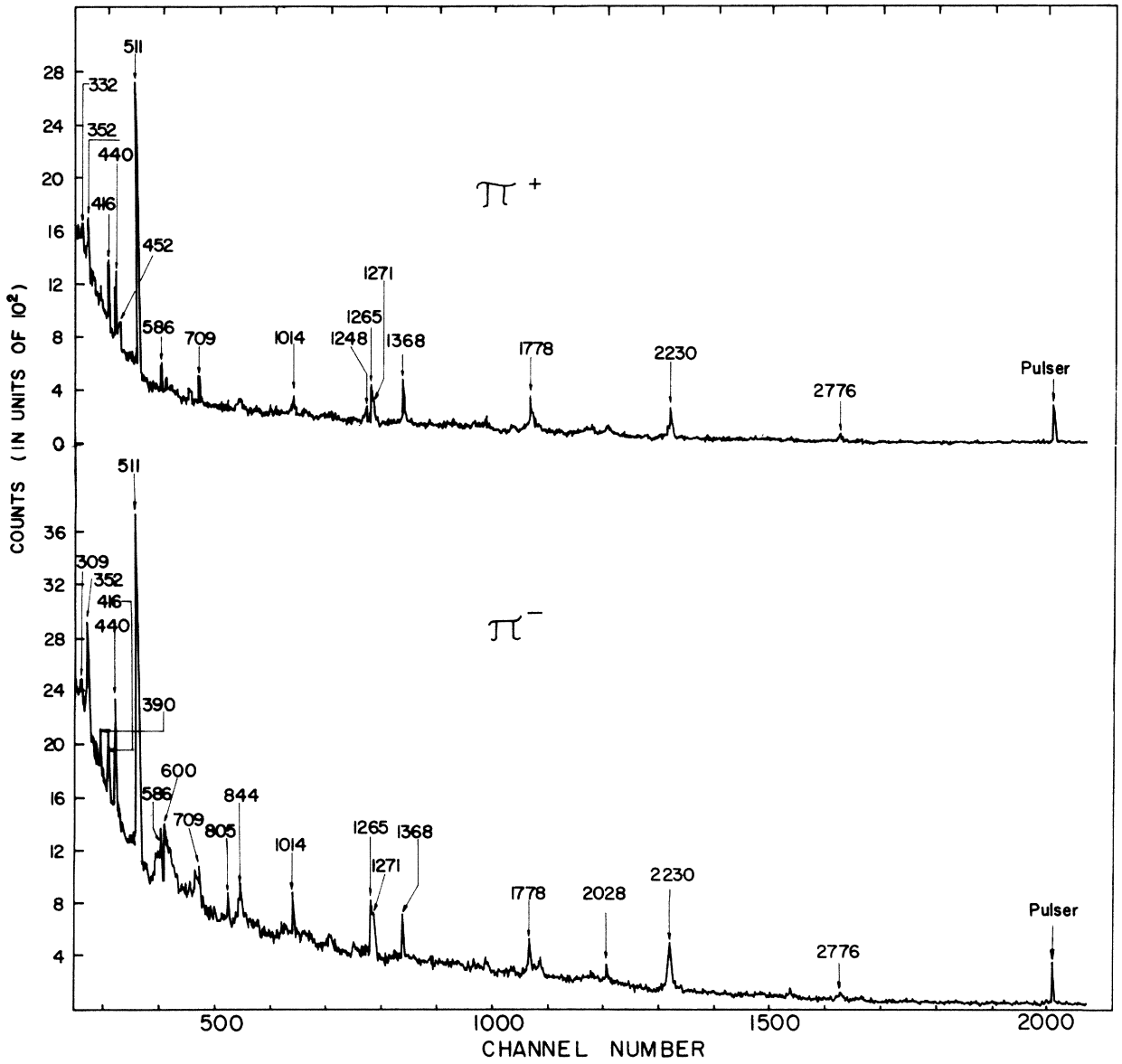

FIG. 3. γ-ray spectra following the interaction of 70-MeV positive pions (top) and negative pions (bottom) with ^{32}S. Measured γ-ray energies are indicated in keV.

IV. DISCUSSION

A. Cascade-evaporation calculations and the prompt γ-ray technique

It is difficult to put in a unified theoretical frame a variety of experimental results such as those obtained in this work. Measured cross sections range from relatively simple reactions, such as charge exchange or knockout, to deep spallation reactions and evaporation processes. The present level of theoretical understanding can hardly explain even simple reactions, let alone a multitude of reactions. On the other hand, the prompt γ-ray technique does not provide enough details to fully test specific theoretical models. We felt that our data could be best interpreted by using Monte Carlo calculations of intranuclear cascades followed by evaporation processes. Such calculations have been successful in correlating a wide range of experimental data obtained for other projectiles. In addition, various intermediate reaction channels and their relative strength can be followed throughout the calculations. There are a few Monte Carlo codes which describe the interactions of pions with nuclei.[15-17] We used the program ISOBAR written by Harp *et al.*,[17] because

TABLE I. Measured and calculated cross sections for the observed γ-ray transitions.

Target nucleus	Removed equiv. particles [a]	Residual nucleus	Transition	E_γ (MeV) Observed	E_γ (MeV) Published [b]	σ_{π^+} (mb) Experiment [c]	IE [d]	σ_{π^-} (mb) Experiment [c]	IE [d]
^{23}Na	–	^{23}Na	I→0	0.439	0.440	20.7 ± 1.0	11.2	32.6 ± 1.6	9.7
	–	^{23}Na	II→0	1.636	1.634	16.4 ± 1.0	3.4	19.4 ± 1.6	2.3
	t	^{20}Ne	I→0		1.634		13.2		14.9
	p	^{22}Ne	I→0	1.275	1.275	16.6 ± 1.0	35.5	23.2 ± 1.4	27.5
	d	^{21}Ne	I→0	0.352	0.350	16.4 ± 0.8	27.0	14.7 ± 0.8	21.6
	^{3}He	^{20}F	I→0	0.654	0.656	0.7 ± 0.6	≤3.7	5.2 ± 0.7	≤9.2
Mg [e]	–	^{24}Mg	I→0	1.369	1.368	42.7 ± 2.2	15.7	21.8 ± 1.1	17.7
	d	^{22}Na	VI→0		1.370		3.9		9.7
	$(\pi^-, 2p)$	^{22}F	II→0		1.360		–		···
	$5p2n$	^{17}N	I→0		1.371		–		0.5
	(π^-, π^0)	^{24}Na	III→I	0.872	0.871	≤2.5	–	3.3 ± 0.7	0.3
	^{7}Be	^{17}O	I→0		0.871		0.5		1.0
	$(\pi^-, 2p)$	^{22}F	I→0	0.658	0.660	≤2.5	–	2.2 ± 0.3	···
	^{4}Li	^{20}F	I→0		0.656		1.0		3.9
	n	^{23}Mg	I→0	0.451	0.451	9.8 ± 0.9	5.6	2.7 ± 0.3	10.2
	p	^{23}Na	I→0	0.439	0.440	15.1 ± 1.1	29.8	10.2 ± 0.5	22.0
	t	^{21}Na	I→0	0.330	0.332	3.1 ± 0.8	1.7	0.3 ± 0.1	2.3
	$2p$	^{22}Ne	I→0	1.274	1.275	8.6 ± 1.4	12.6	8.1 ± 0.5	5.1
	^{3}He	^{21}Ne	I→0	0.350	0.350	11.8 ± 0.9	12.3	7.8 ± 0.4	9.7
	α	^{20}Ne	I→0	1.634	1.634	17.8 ± 2.4	15.4	12.4 ± 0.7	10.2
	^{10}B	^{14}N	II→I		1.632		3.1		4.0
	^{6}Li	^{18}F	I→0	0.937	0.937	6.5 ± 1.1	1.6	2.7 ± 0.4	1.9
^{27}Al	–	^{27}Al	I→0	0.842	0.844	3.6 ± 1.0	3.7	8.3 ± 2.7	0.8
	n	^{26}Al	II→0	0.418	0.417	5.7 ± 0.6	12.7	3.2 ± 2.0	15.2
	p	^{26}Mg	I→0	1.807	1.809	8.9 ± 1.7	54.4	14.1 ± 3.6	26.1
	d	^{25}Mg	I→0	0.585	0.585	3.8 ± 0.8	18.6	8.8 ± 1.8	16.9
	t	^{24}Mg	I→0	1.367	1.369	16.8 ± 1.8	39.1	15.9 ± 3.0	27.2
	^{5}He	^{22}Na	VI→I		1.369		3.5		5.2
	$2n$	^{25}Al	I→0	0.451	0.451	1.4 ± 0.6	0.7	≤4.3	···
	$p3n$	^{23}Mg	I→0		0.451		2.5		···
	α	^{23}Na	I→0	0.441	0.440	13.4 ± 1.0	15.4	19.0 ± 2.1	16.1
	^{5}Li	^{22}Ne	I→0	1.273	1.275	5.0 ± 1.3	6.7	11.1 ± 2.9	17.8
	^{6}Li	^{21}Ne	I→0	0.352	0.351	8.8 ± 1.1	11.9	12.2 ± 3.0	11.5
^{28}Si	–	^{28}Si	I→0	1.777	1.779	12.3 ± 2.8	25.0	22.3 ± 3.0	17.5
	n	^{27}Si	I→0	–	0.780	≤4.4	2.6	≤4.2	6.1
	p	^{27}Al	I→0	0.843	0.844	4.3 ± 1.7	8.3	13.1 ± 2.4	7.2
	d	^{26}Al	II→0	0.417	0.417	7.3 ± 1.5	12.0	8.2 ± 1.6	10.2
	d	^{26}Al	III→I	0.829	0.830	4.2 ± 1.7	15.3	≤4.5	9.6
	t	^{25}Al	I→0	0.452	0.451	6.0 ± 1.6	0.5	≤3.3	0.7
	^{5}He	^{23}Mg	I→0		0.451		3.0		···
	$2p$	^{26}Mg	I→0	1.808	1.809	≤4.4	13.2	15.0 ± 2.7	6.0
	^{3}He	^{25}Mg	I→0	0.585	0.585	8.8 ± 1.5	9.8	12.2 ± 2.0	12.1
	^{5}Li	^{23}Na	I→0	0.440	0.440	9.9 ± 1.7	8.0	17.7 ± 1.9	10.0
	α	^{24}Mg	I→0	1.367	1.369	24.4 ± 3.1	36.3	29.3 ± 3.0	32.9
	^{6}Li	^{22}Na	VI→I		1.369		6.9		4.6
	^{6}Be	^{22}Ne	I→0	1.273	1.275	≤4.6	2.5	10.9 ± 2.2	9.1
	^{7}Be	^{21}Ne	I→0	0.351	0.351	12.4 ± 1.6	7.2	15.9 ± 1.9	10.0
^{31}P	–	^{31}P	I→0	1.266	1.266	53.8 ± 6.5	0.6	32.4 ± 4.7	10.6
	–	^{31}P	II→0	2.234	2.234	34.8 ± 2.5	1.1	46.1 ± 3.6	2.0
	p	^{30}Si	I→0		2.235		40.6		23.1
	d	^{29}Si	II→0	2.027	2.028	12.4 ± 1.7	17.4	22.0 ± 2.8	28.4
	t	^{28}Si	I→0	1.777	1.779	16.9 ± 1.9	41.0	22.0 ± 3.0	32.7
	^{5}He	^{26}Al	II→0	0.418	0.416	7.2 ± 0.8	7.0	6.5 ± 1.1	4.8
	^{6}He	^{25}Al	I→0	0.451	0.451	3.0 ± 0.7	0.2	6.3 ± 1.1	0.8
	^{8}Li	^{23}Mg	I→0		0.451		1.5		

TABLE I. (*Continued*)

Target nucleus	Removed equiv. particles [a]	Residual nucleus	Transition	E_γ (MeV) Observed	E_γ (MeV) Published [b]	σ_{π^+} (mb) Experiment [c]	σ_{π^+} IE [d]	σ_{π^-} (mb) Experiment [c]	σ_{π^-} IE [d]
	^{5}Li	^{26}Mg	I→0	1.807	1.809	4.3 ± 1.5	7.1	27.2 ± 3.1	14.3
	^{6}Li	^{25}Mg	I→0	0.584	0.585	8.1 ± 0.9	7.3	21.0 ± 1.5	5.3
	^{6}Li	^{25}Mg	II→0	0.392	0.390	3.3 ± 0.7	2.7	4.3 ± 1.0	2.2
	^{7}Li	^{24}Mg	I→0	1.366	1.368	22.0 ± 1.7	25.4	16.0 ± 2.3	17.8
	2α	^{23}Na	I→0	0.441	0.440	12.9 ± 0.9	6.9	15.5 ± 1.2	8.7
	^{10}Be	^{21}Na	I→0	0.332	0.332	4.4 ± 0.8	0.8	3.8 ± 0.9	0.3
	^{10}B	^{21}Ne	I→0	0.352	0.350	6.6 ± 0.7	7.9	8.1 ± 1.0	6.5
	^{11}B	^{20}Ne	I→0	1.632	1.634	10.4 ± 1.7	5.0	≤6.3	2.5
	^{17}O	^{14}N	II→I		1.632		0.6		–
^{32}S	–	^{32}S	I→0	2.230	2.230	52.5 ± 2.7	–	75.2 ± 3.8	–
			IV→I		2.229		–		–
	n	^{31}S	II→0		2.232		–		–
	$3p$	^{29}Al	III→0		2.228		–		–
	π^+, π^0	^{32}Cl	III→0	1.265	1.260	21.3 ± 4.4	1.1	–	–
	p	^{31}P	I→0		1.266		23.0	29.5 ± 4.1	12.7
	d	^{30}P	IV→II		1.264		5.1		4.5
	n	^{31}S	I→0	1.248	1.249	9.6 ± 5.1	5.1	≤2.3	15.2
	^{10}Be	^{22}Mg	I→0		1.249		0.5		–
	d	^{30}P	II→0	0.709	0.709	7.3 ± 0.7	7.2	12.5 ± 0.8	6.7
	^{3}He	^{29}Si	I→0	1.271	1.273	12.6 ± 4.2	12.1	13.7 ± 4.2	15.6
	^{3}He	^{29}Si	II→0	2.028	2.028	9.5 ± 3.1	12.0	12.6 ± 1.9	15.5
	α	^{28}Si	I→0	1.778	1.779	17.1 ± 4.0	19.4	27.2 ± 2.4	28.9
	^{6}Li	^{26}Al	II→0	0.416	0.417	6.4 ± 0.6	4.3	3.9 ± 0.6	5.9
	^{7}Li	^{25}Al	I→0	0.451	0.451	5.1 ± 0.7	0.3	≤2.3	0.9
	^{9}Be	^{23}Mg	I→0		0.451		3.4		1.9
	^{7}Be	^{25}Mg	I→0	0.586	0.585	6.8 ± 0.7	7.8	–	7.4
	^{7}Be	^{25}Mg	II→0	0.390	0.390	≤0.9	3.1	1.7 ± 0.5	2.8
	2α	^{24}Mg	I→0	1.368	1.368	29.3 ± 1.5	25.4	21.0 ± 1.2	24.0
	^{10}B	^{22}Na	VI→I		1.369		4.7		2.4
	^{15}F	^{17}N	I→0		1.371		–		–
	^{9}B	^{23}Na	I→0	0.440	0.440	9.9 ± 0.7	7.8	9.2 ± 0.6	11.5
	^{11}C	^{21}Ne	I→0	0.352	0.350	5.6 ± 0.7	5.1	4.8 ± 0.5	8.7
^{39}K	–	^{39}K	II→0	2.813	2.814	11.3 ± 1.5	6.9	20.9 ± 4.3	5.9
	–	^{39}K	IV→II	0.786	0.785	8.5 ± 0.9	0.5	13.1 ± 1.7	0.6
	–	^{39}K	VII→II	1.129	1.130	2.5 ± 1.0	0.1	10.8 ± 3.6	0.2
	$2n$	^{37}K	I→0	1.368	1.369	3.0 ± 1.4	0.2	≤9.3	–
	^{15}N	^{24}Mg	I→0		1.368		7.4		4.4
	^{17}Ne	^{22}F	II→0		1.360		–		
	p	^{38}Ar	I→0	2.166	2.167	23.3 ± 1.5	39.5	37.7 ± 3.7	25.6
	p	^{38}Ar	III→0	1.643	1.643	9.1 ± 1.3	17.5	16.9 ± 3.3	10.0
	p	^{38}Ar	V→III	0.670	0.669	7.4 ± 0.9	10.3	10.7 ± 1.4	3.3
	d	^{37}Ar	II→0	1.610	1.611	7.9 ± 1.3	10.1	14.8 ± 4.0	10.0
	^{14}N	^{25}Mg	III→0		1.611		0.1		0.3
	t	^{36}Ar	I→0	1.968	1.970	Large [f]	17.5	13.2 ± 4.8	12.4
	^{13}B	^{25}Si	III→0		1.963		–		–
	^{5}He	^{34}Cl	II→0	0.461	0.461	2.8 ± 0.8	3.0	2.4 ± 1.7	1.5
	^{5}Li	^{34}S	I→0	2.127	2.127	12.1 ± 3.0	15.1	23.0 ± 4.6	20.3
	^{9}Be	^{30}P	II→0	0.711	0.709	7.8 ± 3.4	5.8	44.9 ± 5.1	1.3
	^{13}C	^{26}Al	II→0	0.417	0.417	≤1.5	2.3	3.1 ± 1.2	1.0
	^{15}O	^{24}Na	III→I	0.872	0.869	≤0.8	0.1	5.3 ± 2.8	0.2
			V→I		0.874		–		–
	^{22}Na	^{17}O	I→0		0.871		–		–
	4α	^{23}Na	I→0	0.440	0.440	0.6 ± 0.3	0.3	6.5 ± 1.3	1.3
	^{18}F	^{21}Ne	I→0	0.348	0.350	≤1.2	0.6	3.6 ± 1.2	0.6
	^{19}Ne	^{20}F	II→0	0.821	0.823	3.3 ± 0.8	1.2	≤9.1	1.2
	^{14}B	^{25}Si	II→0		0.815		–		–

TABLE I. (*Continued*)

Target nucleus	Removed equiv. particles [a]	Residual nucleus	Transition	E_γ (MeV) Observed	E_γ (MeV) Published [b]	σ_{γ^+} (mb) Experiment [c]	σ_{γ^+} (mb) IE [d]	σ_{γ^-} (mb) Experiment [c]	σ_{γ^-} (mb) IE [d]
^{40}Ca	–	^{40}Ca	II→0	3.737	3.737	8.5 ± 1.0	15.4	19.1 ± 2.5	11.3
	–	^{40}Ca	IV→II	0.753	0.754	4.4 ± 0.5	11.2	6.0 ± 1.1	8.3
	π^-, 2p	^{38}Cl	II→0		0.755	–	–		–
	^{9}C	^{31}Si	I→0		0.753		–		0.6
	π^-, π^0	^{40}K	IV→I	1.612	1.613	–	–	21.9 ± 2.2	–
	^{3}He	^{37}Ar	II→0		1.611	6.0 ± 0.8	7.7		12.1
	^{15}N	^{25}Al	III→0		1.612		0.6		0.6
	^{15}O	^{25}Mg	III→0		1.612		0.6		0.8
	d	^{38}K	II→I	0.332	0.330	6.6 ± 0.5	16.9	9.3 ± 0.9	16.7
	^{19}F	^{21}Na	I→0		0.332		–		0.6
	2p	^{38}Ar	I→0	2.168	2.168	9.6 ± 1.5	20.7	16.3 ± 2.6	22.2
	α	^{36}Ar	I→0	1.972	1.970	22.6 ± 2.1	16.2	16.4 ± 3.4	12.0
	^{4}Li	^{36}Cl	I→0	0.789	0.789	4.4 ± 0.6	1.4	46.2 ± 2.3	8.4
	^{6}Li	^{34}Cl	II→0	0.463	0.461	2.0 ± 0.4	6.4	≤2.1	3.3

[a] This indicates the cluster or corresponding group of individual nucleons removed in the reaction, assuming inelastic pion scattering.

[b] The criteria for assigning transitions to the observed γ-ray energy are that the observed and known energies agree to within 2 keV uncertainty in the energy calibration and the uncertainty in the published values.

[c] Errors given are due to statistics, the uncertainty in the energy dependence of the detector efficiency, background subtraction, and ambiguity in doublets decomposition. In addition, the uncertainty in the absolute cross sections is 15%. For some of the lines, the cross sections include contributions from secondary reactions (see Sec. III of text).

[d] Cross sections for the observed γ transition calculated with the modified ISOBAR-EVA code (IE).

[e] The "removed equivalent particles" for Mg, assumes an interaction with ^{24}Mg, whose abundance in the target was 79%.

[f] This peak had an unusual shape and was assumed to be unresolved from surrounding background. Hence, the cross section is not given.

it includes assumptions made by the other authors, together with a more detailed treatment of the various aspects of the pion-nucleus cascade interaction. In this code, the pion-nucleus interaction is described by sequential two-body scatterings of pions and nucleons in the nucleus. A π-N interaction can result in the production of a Δ isobar. Such an isobar can then interact with nucleons and can also subsequently decay. The program uses measured pion-nucleon and nucleon-nucleon cross sections to describe the different two-body scatterings. The nuclear density is taken from electron scattering. As a result of these interactions called "intranuclear cascades," a few particles are emitted and a residual nucleus is usually left in an excited state. The ISOBAR code calculates for each cascade the identity, the mass, the momentum, the energy, and the direction cosines of the emitted particles and of the corresponding residual nucleus. We used recommended[17] ISOBAR options in which: (1) pions and nucleons are not reflected or refracted at the nuclear surface, (2) the pion-nucleus potential was taken to be -25 MeV, (3) Δ-nucleon charge-exchange scatterings are not allowed, and (4) no restriction is made on the distance between successive collision sites.

The output of ISOBAR is fed as an input into the computer code EVA[18] which simulates nuclear evaporation processes from the excited residual nuclei produced in the intranuclear-cascade stage. Each ISOBAR-EVA calculation consisted of 1000 ISOBAR events, followed by two EVA evaporations for each ISOBAR event. The statistical uncertainties in these calculations are about 20% for a 20-mb cross section.

Whenever such calculations are used for the interpretation of experimental results obtained by the prompt γ-ray technique, they should not be used directly for reasons explained below. As was previously mentioned, the cross section obtained in a prompt γ-ray experiment is a measure of the production of a specific excited state in the residual nucleus. This includes therefore contributions from higher excited states (populated in the same reaction) which decay with appropiate branching ratios to the observed state. One should extract from the calculated total cross section for reaching a specific residual nucleus the fraction corresponding to the measured level. This was done in the following way: The ISOBAR-EVA (IE) calculations yield, for each residual nucleus, the probability for leaving it at a certain excitation energy. The known energy level scheme of each

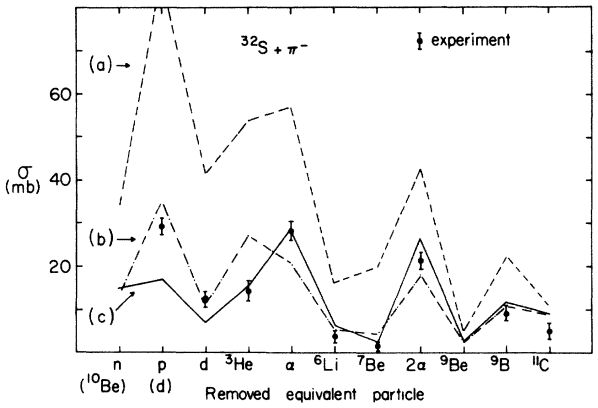

FIG. 4. Comparison between experiment and ISOBAR-EVA calculations: (a) unmodified, (b) modified to take into account the known energy levels and branching ratios, (c) same as (b) with the inclusion of the δ modification (see Sec. IV A). The lines between calculated points are drawn only to guide the eye.

residual nucleus[12] was divided into regions of 0.5-MeV width. A weight was assigned to each region according to the calculated probability for leaving the nucleus at that region of excitation energy. This weight was equally distributed among the excited states located in that region, and their contribution to the observed transition was then calculated, using the known branching ratios.[12] The effect of this correction is large, as shown in Fig. 4. Whenever transitions in two or more nuclei correspond to the same measured energy, the strongest cross section (according to calculations) is mentioned first and the others are given in parentheses (see Fig. 4).

One difficulty in the above procedure is that the EVA calculations introduce distortions in the probability for leaving the residual nucleus at a certain excitation energy. As a first consequence, nuclei which were energetically allowed to decay further by particle emission are artificially kept as "stable" due to the specific way in which the integrated emission widths are calculated. Pairing and closed shell effects are taken into account[18] by displacing upward the ground state of certain nuclei by the pairing energy δ, typically about 1 MeV. In this way, the emission widths, which are proportional to the density of states in the final nuclei, are adjusted to fit a more realistic picture of the nuclear structure. Kinematically, a nucleus A with a separation energy Q for the emission of a certain particle leading to nucleus B will need an excitation energy larger than $Q+\delta$ in order to decay by particle emission. Here, δ is the displacement of the ground state in the nucleus B. Thus, nucleus A with excitation energy between Q and $Q+\delta$ is closed to particle decay. This does not affect considerably the total cross section for production of the nucleus A (as measured for example in activation analysis) due to a compensating effect. The nucleus A which is not allowed to decay further, whenever its excitation energy is between Q and $Q+\delta$, is not itself populated strongly from the decay of neighboring nuclei. A second consequence of the distortions introduced by the EVA code is that the relative population of the low excited states in the nucleus B will be reduced. The cross sections calculated in the EVA code will therefore not be appropriate for comparison with results of prompt γ-ray experiments. We modified the EVA code so that nuclei left in the region between Q and $Q+\delta$ can nonetheless decay by particle emission (this was done by setting $\delta = 0$). For excitation energies above $Q+\delta$, the δ values were not changed. The effect of this modification may be seen in Fig. 4. There are some changes in the absolute cross sections, especially for reactions in which few nucleons are removed. For instance, the ratio of "^{3}He" to "α" removal cross sections agrees better with experiment.

B. Results of modified calculations

Figures 5 and 6 present some of the measured results compared with calculated cross sections. For each figure, the abscissa refers to the removed equivalent particles which will bring the target to the observed final nucleus. The agreement between calculated and measured cross sections is good. It should be emphasized that no normalization parameter has been used in the calculation. A closer examination of the results for each target allows us to distinguish between two groups. Apart from a few cases there is generally good agreement for residual nuclei reached through the removal of many nucleons and poor agreement for residual nuclei reached through the removal of few nucleons (up to about three). A possible explanation for this difference is the following: Whereas products far from the target nucleus are reached essentially by evaporation (calculated by the EVA code), most of the nuclei reached through the removal of a few nucleons are produced in the pre-equilibrium stage of the reaction (calculated by the ISOBAR code). The EVA code has a well understood theoretical basis and its results have been checked against a large amount of experimental data. This is not the case for the ISOBAR code, which is affected by the present scarcity of data for pion induced reactions and by the relatively poor understanding of the pion-nucleus interaction.

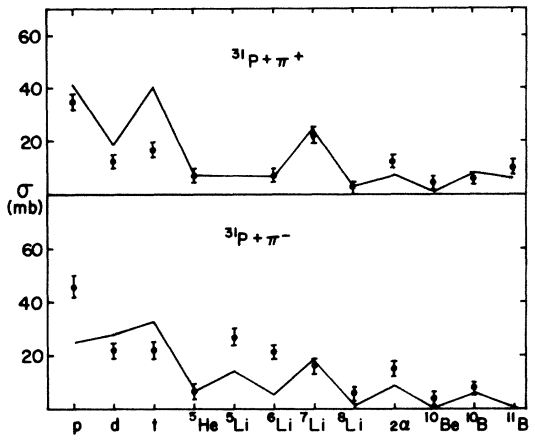

FIG. 5. Comparison of the modified ISOBAR-EVA calculations with prompt γ-ray results obtained in the present work for ^{31}P. The lines between calculated points are drawn only to guide the eye.

C. Single-nucleon-removal reactions

These reactions have been previously studied over the pion energy of 50 to 1900 MeV.[1-6] Most published data on these reactions consist of cross sections measured through the radioactivity of the residual nuclei. Particular attention has been devoted to cross-section ratios of the type

$$R_1(A) = \frac{\sigma[A(\pi^-, \pi^- n)B]}{\sigma[A(\pi^+, \pi^+ n + \pi^0 p)B]}$$

and

$$R_2(A) = \frac{\sigma[A(\pi^+, \pi^+ p)C]}{\sigma[A(\pi^-, \pi^- p + \pi^0 n)C]}$$

which have been found in most cases to deviate

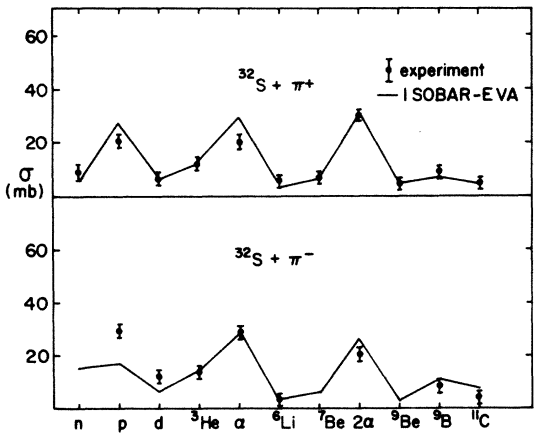

FIG. 6. Comparison of the modified ISOBAR-EVA calculations with prompt γ-ray results obtained in the present work for ^{32}S. The lines between calculated points are drawn only to guide the eye.

significantly from predictions of simple impulse approximations. Many attempts have been made to understand these ratios including modified plane wave impulse approximation (PWIA) calculations,[19] cascade calculations,[6,20] effects of final-state interation,[21] and effects of the giant dipole resonance as an intermediate state in the reaction.[22] Sternheim and Silbar[23] suggested recently that the inclusion in the calculation of enhanced nucleon charge exchange may improve the agreement with the experimental results.

About 20 cross sections for transitions which correspond to one nucleon removal were measured in the present work. The observed ratios $R_2(A)$ are presented in Table II together with simple impulse-approximation (IA) predictions, calculated from pion-nucleon cross sections at 70 MeV,[24] and the results of the IE cascade-evaporation calculations. All measured ratios disagree with the impulse-approximation predictions, indicating that a more sophisticated approach is needed for the analysis of the reactions. Although the cascade-evaporation calculations come closer to the measured values, they still overestimate the ratios by a factor of 2 or more. By using the phenomenological model proposed by Sternheim and Silbar[23] we were able to reproduce the measured ratios with values of P (measures the probability for nucleon charge exchange) of about 0.4. This is below the maximum allowed value of $P = 0.5$ and larger than $P = 0.25$ calculated for ^{12}C at $E_\pi = 180$ MeV. Still, this model is unable to explain the measured ratios:

$$R_3(A) = \frac{\sigma[A(\pi^-, \pi^- p + \pi^0 n)C]}{\sigma[A(\pi^+, \pi^+ n + \pi^0 p)B]} .$$

Experimental results for this ratio, together with the corresponding IE results, are listed in Table II. When A is a $T = 0$ nucleus, then B and C are mirror nuclei and there is complete isospin symmetry between numerator and denominator. We therefore expect this ratio to be of the order of unity (a small difference from unity is expected because of Coulomb effects in the incoming channel). The observed ratio for ^{28}Si and ^{32}S are larger than 3. We considered two possible reaction mechanisms through which a large asymmetry may be introduced in this reaction. The first mechanism may be observed through a detailed analysis of the IE calculations (which reproduce these ratios reasonaly well). In these $T = 0$ nuclei, the threshold for neutron emission is higher by about 5 MeV than for proton emission. A large fraction of the cross section comes from inelastic pion scattering followed by nucleon evaporation. If these inelastic scattering process strongly populated unbound levels

TABLE II. Experimental and theoretical cross section ratios of single-nucleon-removal reactions.

Target nucleus	$R_2(A)$ Experimental	$R_2(A)$ IE[a]	$R_2(A)$ IA[b]	$R_3(A)$ Experimental	$R_3(A)$ IE[a]	$\frac{\sigma(\gamma,p)}{\sigma(\gamma,n)}$[c]
^{23}Na	0.71 ± 0.07	1.3	2.1			
^{27}Al	0.6 ± 0.2	2.1	2.1			
^{28}Si	0.3 ± 0.1	1.1	2.1	≥3.0 ± 0.6	2.8	3.9
^{31}P	0.75 ± 0.1	1.8	2.1			
^{32}S	0.72 ± 0.06	1.4	2.1	3.1 ± 0.5	2.2	4.6
^{39}K	0.62 ± 0.08	1.5	2.1			

[a] Cross-section ratios calculated with the modified ISOBAR-EVA code.
[b] Impulse-approximation predictions. See Sec. IV C.
[c] From S.A.E. Johansson (Ref. 26).

at excitation energies below the neutron emission threshold, an asymmetry is introduced in the nucleon evaporation rate, favoring proton emission. The second mechanism is based on the suggestion[22] that the giant dipole resonance (GDR) may play an important role in these reactions. If the first step of the reactions populates strongly the GDR, an asymmetry in the nucleon emission rate is then introduced through isospin mixing,[25] again favoring proton emission. It is interesting to note that measured ratios of (γ,p) to (γ,n) cross sections in the region of the GDR[26] (listed in Table II) are very similar to the $R_3(A)$ ratios measured in the present work.

An interesting situation arises by the recent measurement[5] of cross sections on ^{16}O at $E_\pi = 180$ MeV, where the measured R_3 ratio is unity. This value can be understood in the framework of the cascade evaporation model, since the IE calculations show that at high energies the probability of exciting the region between proton and neutron emission thresholds is small, so that no appreciable deviation from unity is expected. On the other hand, the ratio of (γ,p) to (γ,n) cross sections for ^{16}O is also unity. It thus appears that even this case cannot be used to determine the relative merits of the two explanations given above for the asymmetry of cross sections ($R_3 \neq 1$) for several $T = 0$ targets.

D. α removal reactions

Most of the reported γ-ray experiments with pions[2] (and also kaons[27]) emphasize the large cross sections observed for the removal of one or more α clusters from even-even nuclei. Several mechanisms, some of them involving the existence of α clusters on the nuclear surface, were proposed[28] to explain these large cross sections. In the present work large cross sections for reactions involving the removal of one or several α clusters from even-even nuclei were also observed. The cascade-evaporation calculations which we performed, including the modifications described above, reproduced well the measured cross sections. These calculations do not include any clustering effects in the intranuclear-cascade stage (ISOBAR code) but allow for the evaporation of α particles after the pre-equilibrium stage has been reached. This agreement suggests that the large cross sections may be understood within the framework of an evaporation model, and are due mainly to Q value effects and to the decay schemes of even nuclei which favor decay to the 0^+ ground state through the $2^+ \rightarrow 0^+$ observed transition. This last effect is explicitly taken into account in our calculations. As may be seen from Table I, the cross section for t removal from a $T = \frac{1}{2}$ target nucleus is about as large as for α removal from the adjacent $T = 0$ target nucleus. This suggests that the final nucleus, rather than the removed particle, is mainly responsible for the observed strength.

E. Evaporation and absorption processes

In Fig. 7 the cross sections for the production of some final nuclei are plotted for four different targets. As can be seen, the residual nuclei are produced with similar cross sections irrespective of the target nucleus. This feature is characteristic of an evaporation process. A similar feature is observed in Fig. 8, where we present cross sections for the same γ-ray transitions for the interaction with ^{27}Al of 70-MeV positive pions (present work), 80-MeV ^{3}He,[29] and 190-MeV protons[30] all done with the prompt γ-ray technique. The residual nuclei are produced with a similar pattern. Again, this is characteristic of an evaporation process with takes place after a pre-equilibrium stage has been reached.

It is interesting to note that the IE calculations

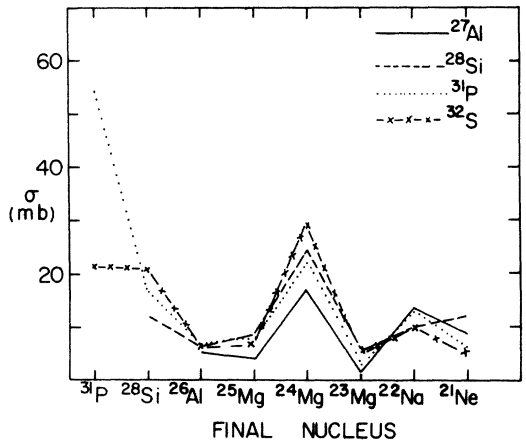

FIG. 7. Measured cross sections for the production of the same final nuclei following the interaction of 70-MeV π^- with ^{27}Al, ^{28}Si, ^{31}P, and ^{32}S. Lines through the measured cross sections are drawn only to guide the eye.

show that a large fraction (50% or more) of the cross sections for reactions resulting in the removal of four or more nucleons comes from processes in which a pion was absorbed in flight. Some asymmetries in the production of the same residual nucleus from the same target by positive or negative pions could possibly be explained if one assumes an absorption process. For example, the production of ^{36}Cl from a ^{40}Ca target could be interpreted as ^{4}Li removal for a nonabsorptive process. If absorption took place, an α cluster would be removed for π^- absorption and four protons for π^+ absorption. We observe a large asymmetry for ^{36}Cl production $[\sigma(\pi^-)/(\sigma(\pi^+) \approx 11]$. This asymmetry may indicate the importance of absorption, since the probability of α evaporation is larger than the probability for the successive evaporation of four protons. The IE calculation for the ^{36}Cl yield predicts a large asymmetry related to the fact that the π^- IE calculated cross section comes mainly from pion absorption. Previously, Ullrich *et al.*[1] concluded that the absorption of pions in flight is an important component in the interaction of 60-MeV pions with nuclei.

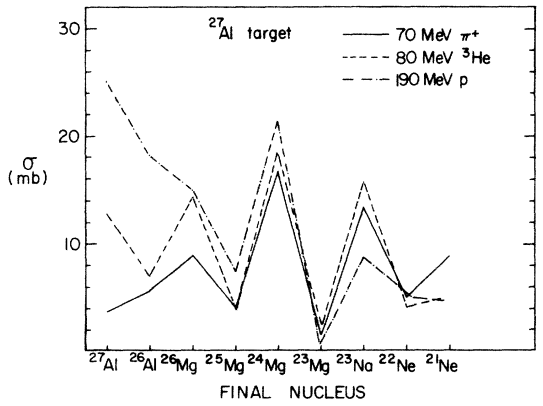

FIG. 8. Measured prompt γ-ray cross sections following the interaction of 70-MeV π^+ (present work), 80-MeV ^{3}He (Ref. 29), and 190-MeV protons (Ref. 30) with ^{27}Al. The results of the two last works are given with arbitrary normalization. Lines through experimental points are drawn only to guide the eye.

CONCLUSIONS

The experimental results obtained in the present work and their interpretation through the ISOBAR-EVA calculation support the following conclusions:

(a) Pion induced spallation reactions could be well understood in terms of evaporation processes. Evaporation calculations account for the measured cross sections in both absolute and relative values. The fact that different targets or projectiles generate similar distributions of residual nuclei is a further indication that evaporation processes dominate the multinucleon removal reactions induced by 70-MeV pions.

(b) Single-nucleon-removal reactions cannot be understood using only a quasifree interaction mechanism or the present cascade-evaporation calculations. Comparison of various π^+ and π^- induced reaction cross sections with calculations suggests that other processes such as pion inelastic scattering followed by nucleon emission, intermediate states such as the giant dipole resonance, or nucleon charge exchange within the nucleus should be considered in order to reproduce correctly the experimental results.

(c) α-removal cross sections, previously noted for their large relative magnitude in the pion-nucleus interactions, were well understood in the framework of an evaporation model. These processes, generally strong for $T = 0$ targets, were found to be very similar in magnitude to t removal reactions in neighboring $T = \frac{1}{2}$ targets, and this similarity indicates that the residual nucleus rather than the removed particle is mainly responsible for the observed strength. In addition, the present cascade-evaporation calculations indicate that about 50% of the α removal processes are a result of in-flight pion absorption.

(d) Absorption mechanisms dominate the calculated cross section for the removal of many nucleons (4 or more). Some asymmetries in the cross section of reactions induced by π^+ and π^- projectiles leading to the same residual nucleus may be understood if an absorptive process is assumed.

ACKNOWLEDGMENT

We wish to thank Dr. Ph. Catillon, Dr. F. Netter, and Dr. J. Julien and the Saclay Laboratory personnel for their help and assistance in carrying out the experiments. Many helpful discussions with Dr. Z. Fraenkel and Dr. J. Ginocchio are gratefully acknowledged. We also appreciate the skillful technical assistance of Mr. M. Zilca.

---

*Work supported in part by the Israeli Academy of Sciences and Humanities.

†Present address: Los Alamos Scientific Laboratory, University of California, Los Alamos, New Mexico 87545.

[1]H. Ullrich, E. T. Boschitz, H. D. Engelhardt, and C. W. Lewis, Phys. Rev. Lett. 33, 433 (1974)

[2]V. G. Lind, H. S. Plendl, H. O. Funsten, W. J. Kossler, B. J. Lieb, W. F. Lankford, and A. J. Buffa, Phys. Rev. Lett. 32, 479 (1974).

[3]R. E. Segel, L. R. Greenwood, P. Debevec, H. E. Jackson, D. G. Kovar, L. Meyer-Schützmeister, J. E. Monahan, F. J. D. Serduke, T. P. Wangler, W. R. Wharton, and B. Zeidman, Phys. Rev. C 13, 1566 (1976).

[4]D. Ashery, M. Zaider, Y. Shamai, S. Cochavi, M. A. Moinester, A. I. Yavin, and J. Alster, Phys. Rev. Lett. 32, 943 (1974).

[5]B. J. Lieb, H. S. Plendl, H. O. Funsten, W. J. Kossler, and C. E. Stronach, Phys. Rev. Lett. 34, 965 (1975).

[6]M. A. Moinester, M. Zaider, J. Alster, D. Ashery, S. Cochavi, and A. I. Yavin, Phys. Rev. C 8, 2039 (1973), and references therein.

[7]H. E. Jackson, D. G. Kovar, L. Meyer-Schützmeister, R. E. Segel, J. P. Schiffer, S. Vigdor, T. P. Wangler, R. L. Burman, D. M. Drake, P. A. M. Gram, R. P. Redwine, V. G. Lind, E. N. Hatch, O. H. Otteson, R. E. McAdams, B. C. Cook, and R. B. Clark, Phys. Rev. Lett. 35, 641 (1975).

[8]B. J. Lieb, W. F. Lankford, S. H. Dam, H. S. Plendl, H. O. Funsten, W. J. Kossler, V. G. Lind, and A. J. Buffa, Phys. Rev. C 14, 1515 (1976).

[9]P. Y. Bertin, J. Berthot, B. Bihoreau, G. Collin, J. Duclos, A. Gerard, D. Isabelle, A. Magnon, A. Arthur, J. Miller, J. More, J. Morgenstern, P. Nemethy, A. Planchard, and L. Roussel, Saclay report, 1971 (unpublished).

[10]H. E. Jackson, D. G. Kovar, L. Meyer-Schützmeister, S. E. Vigdor, T. P. Wangler, R. E. Segel, J. P. Schiffer, R. L. Burman, P. A. M. Gram, D. M. Drake, V. G. Lind, E. N. Hatch, O. H. Otteson, R. E. McAdams, B. C. Cook, and R. B. Clark, Phys. Rev. Lett. 35, 1170 (1975).

[11]M. Zaider, Ph.D. thesis, Tel-Aviv University, Israel (unpublished).

[12]P. M. Endt and C. van der Leun, Nucl. Phys. A214, 1 (1973); R. J. Meijer, H. S. Plendl, and R. Holub, At. Data Nucl. Data Tables 13, 1 (1974), Tables for Prompt Gamma Ray Spectroscopy, Part I, $A = 6$ to $A = 20$; R. J. Meijer, A. G. Drentje, and H. S. Plendl, *ibid.* 15, 391 (1975). Tables for Reaction Gamma Ray Spectroscopy, Part II, $A = 21$ to $A = 32$.

[13]N. Yanaki, M.Sc. thesis, Tel-Aviv University, Israel (unpublished).

[14]W. J. Kossler and R. R. Silbar, Los Alamos Scientific Laboratory report No. LA-UR-75-1131 (unpublished).

[15]N. Metropolis, R. Bivins, M. Storm, A. Turkevitch, J. M. Miller, and G. Friedlander, Phys. Rev. 110, 185 (1958); N. Metropolis, R. Bivins, M. Storm, J. M. Miller, G. Friedlander, and A. Turkevitch, ibid. 110, 204 (1958).

[16]H. W. Bertini, Phys. Rev. 171, 1261 (1968).

[17]G. D. Harp, K. Chen, G. Friedlander, Z. Fraenkel, and J. M. Miller, Phys. Rev. C 8, 581 (1973).

[18]I. Dostrovski, Z. Fraenkel, and G. Friedlander, Phys. Rev. 116, 683 (1959).

[19]V. M. Kolybasov, Yad. Fiz. 2, 144 (1965) [Sov. J. Nucl. Phys. 2, 101 (1966)].

[20]H. W. Bertini, Phys. Rev. 131, 1801 (1963).

[21]P. W. Hewson, Nucl. Phys. A133, 659 (1969); D. Robson, Ann. Phys. (N.Y.) 71, 277 (1972).

[22]D. H. Wilkinson, in *Proceedings of the International Conference on Nuclear Structure, Tokyo, 1967,* edited by J. Sawada (Univ. of Tokyo Press, Tokyo, Japan, 1967), p. 469; G. L. Strobel, Nucl. Phys. A232, 502 (1974).

[23]M. M. Sternheim and R. R. Silbar, Phys. Rev. Lett. 34, 824 (1975); R. R. Silbar, J. N. Ginocchio, and M. M. Sternheim, Phys. Rev. C 15, 371 (1977).

[24]G. Giacomelli, P. Pini, and S. Stagni, CERN Report No. CERN-HERA 69-1, 1969 (unpublished); A. A. Carter, J. R. Williams, D. V. Bugg, P. J. Bussey, and D. R. Dance, Nucl. Phys. B26, 445 (1971).

[25]F. C. Barker and A. K. Mann, Phil, Mag. 2, 5 (1957).

[26]S. A. E. Johansson, Phys. Rev. 97, 1186 (1955).

[27]P. D. Barnes, R. A. Eisenstein, W. C. Lam, J. Miller, R. B. Sutton, M. Eckhause, J. Kane, R. E. Welsh, D. A. Jenkins, R. J. Powers, R. Kunselman, R. P. Redwine, R. E. Segel, and J. P. Schiffer, Phys. Rev. Lett. 29, 230 (1972).

[28]V. G. Lind, H. O. Funsten, H. S. Plendl, W. F. Lankford, and W. J. Buffa, Bull. Am. Phys. Soc. 17, 918 (1972).

[29]P. P. Singh, M. Sadler, A. Nadasen, L. A. Beach, and C. R. Gossett, Phys. Rev. C 14, 1655 (1976).

[30]O. Artun, Y. Cassagnou, R. Legrain, N. Lisbona, L. Roussel, J. P. Alard, A. Baldit, J. P. Costilhes, J. Fargeix, G. Roche, and J. C. Tamain, Phys. Rev. Lett. 35, 773 (1975).